^{1}H NMR (CCl_4/C_6H_6) δ 2.10 (s, 1 H, OH), 4.27 (m, 1 H, -C*H*(OH)), and 5.10-6.55 (m, 6 H, CH=CH_2).

Anal. Calcd for $C_6H_8F_2O$: C, 53.73; H, 6.01. Found: C, 53.66; H, 6.25.

Also formed was CH_2=CHCH(OH)C_4H_9-*n*, n^{20}_D, 1.4333 (lit.[25] n^{20}_D 1.4337), in 51% yield.

^{1}H NMR (CCl_4/C_6H_6) δ 0.63-1.57 (m, 9 H, C_4H_9), 1.70 (s, 1 H, OH), 3.97 (m, 1 H, -C*H*(OH)), and 4.73-6.06 (m, 3 H, CH=CH_2).

(7) **PhCH(OH)CF_2CH=CH_2**, n^{25}_D 1.5008, from 6 mmol of CH_2=CHCF_2Br, 12 mmol of benzaldehyde, and 7 mmol of *n*-butyllithium in 15% yield.

^{1}H NMR ($CDCl_3$) δ 2.4 (s, 1 H, OH), 4.9 (t, *J* = 8 Hz, 1 H, $CHCF_2$), 5.25-6.3 (m, 3 H, CH=CH_2), and 7.4 (m, 5 H, Ph).

Anal. Calcd for $C_{10}H_{10}F_2O$: C, 65.2; H, 5.43. Found: C, 64.9; H, 5.62.

In another experiment, PhCH(OH)C_4H_9-*n* also was identified (78%) and isolated; n^{20}_D 1.5083 (lit.[26] n^{20}_D 1.5078).

^{1}H NMR (CCl_4/Me_4Si) δ 0.9-1.9 (m, 10 H, C_4H_9 and OH), 4.6 (t, ^3J(H-H) = 7 Hz, 1 H, PhC*H*), and 7.2 (s, 5 H, Ph).

Reactions of *gem*-(Difluoroallyl)lithium with Esters. The reaction of *gem*-(difluoroallyl)lithium with methyl chloroacetate is typical.

The standard apparatus was charged with 80 mL of THF, 1.68 g (10.7 mmol) of CH_2=$CHCF_2Br$, 3.02 g (27.8 mmol) of methyl chloroacetate, 20 mL of diethyl ether, and 20 mL of pentane. This mixture was cooled to -95 °C and 4.5 mL (10 mmol) of 2.3 M *n*-butyllithium in hexane was added dropwise, very slowly. Upon completion of the addition the reaction mixture was stirred at -95 °C for 90 min and subsequently was allowed to warm slowly to room temperature. Hydrolysis with saturated aqueous NH_4Cl and work up as in the other experiments followed. GLC analysis of the organic residue (15% QF-1 on Chromosorb W, 100 °C) showed the presence of $ClCH_2C(O)CF_2CH$=CH_2, n^{20}_D 1.4122, in 95% yield.

^{1}H NMR(CCl_4/C_6H_6) δ 4.10 (s, 2 H, $ClCH_2$) and 5.50-5.82 (m, 3 H, CH=CH_2); IR (thin film) ν(C=O) 1752 cm^{-1}.

Anal. Calcd for $C_5H_5ClF_2O$: C, 38.86; H, 3.26. Found: C, 39.21; H, 3.50.

The following were prepared by this procedure.

(1) $(CH_3)_2$CHC(O)CF_2CH=CH_2, n^{25}_D 1.3792, from 11.5 mmol of CH_2=$CHCF_2Br$, 30.1 mmol of $(CH_3)_2CHCO_2CH_3$, and 10 mmol of *n*-butyllithium, in 62% yield.

^{1}H NMR (CCl_4/C_6H_6) δ 1.21 (d, ^3J(H-H) = 7 Hz, 6 H, CH_3), 3.13 (sept, ^3J(H-H) = 7 Hz, 1 H, Me_2CH), and 5.38-6.27 (m, 3 H, CH=CH_2); IR (thin film) ν(C=O) 1740 cm^{-1}.

Anal. Calcd for $C_7H_{10}F_2O$: C, 56.75; H, 6.80. Found: C, 56.75; H, 6.90.

(2) $(CH_3)_3$CC(O)CF_2CH=CH_2, n^{25}_D 1.3902, from 16.0 mmol of CH_2=$CHCF_2Br$, 20.3 mmol of $(CH_3)_3CCO_2CH_3$, and 15 mmol of *n*-butyllithium, in 49% yield.

^{1}H NMR (CCl_4/C_6H_6) δ 1.30 (t, ^5J(H-F) = 0.8 Hz, 9 H, CH_3) and 5.36-6.13 (m, 3 H, CH=CH_2); IR (thin film) ν(C=O) 1730 cm^{-1}.

Anal. Calcd for $C_8H_{12}F_2O$: C, 59.25; H, 7.46. Found: C, 59.26; H, 7.49.

Reaction of Methyl Chloroacetate with 2 Molar Equiv of *gem*-(Difluoroallyl)lithium. Using the usual procedure, 4.1 mL of 2.4 M *n*-BuLi (9.8 mmol) in hexane was added dropwise, very slowly, to a solution of 4.50 g (28.7 mmol) of CH_2=$CHCF_2Br$ is 80 mL of THF, 20 mL of diethyl ether, and 20 mL of pentane. The resulting mixture was stirred at -95 °C for 60 min and then 4.5 mL (11 mmol) of *n*-BuLi solution was added. After the reaction mixture had been stirred for another 60 min, 2.5 mL (20 mmol) of Me_3SiCl was added at -95 °C and then the mixture was stirred and allowed to warm slowly to room temperature. After trap-to-trap distillation (70 °C, 0.10 mmHg) into a liquid nitrogen cooled receiver and concentration of the volatiles at reduced pressure, GLC analysis of the liquid residue showed the presence of a major product which was identified as $ClCH_2C(OMe)(OSiMe_3)CF_2CH$=$CH_2$ (36% yield), n^{20}_D 1.42222.

^{1}H NMR (CCl_4/C_6H_6) δ 0.16 (s, 9 H, $SiMe_3$), 3.41 (s, 3 H, OMe), 3.67 (s, 2 H, $ClCH_2$), and 5.30-6.10 (m, 3 H, CH=CH_2).

Anal. Calcd for $C_9H_{17}ClF_2O_2Si$: C, 41.77; H, 6.62. Found: C, 42.02; H, 6.65.

Acknowledgment. This work was supported in part by the U.S. Office of Naval Research.

(25) Grayson, J. T.; Greenlee, K. W.; Derfer, J. M.; Boord, C. E. *J. Org. Chem.* **1955**, *20*, 275.

(26) Ipatieff, V. N.; Haensel,V. *J. Am. Chem. Soc.* **1942**, *64*, 520.

Comparison of Radiationless Decay Processes in Osmium and Platinum Porphyrins

Glauco Ponterini,[†1] Nick Serpone,[‡] Michael A. Bergkamp,[†] and Thomas L. Netzel*[†]

Contribution from the Departments of Chemistry, Brookhaven National Laboratory, Upton, New York 11973, and C.P.L.F.P. Centre, Concordia University, Montreal, Canada H3G-1M8. *Received October 12, 1982*

Abstract: Two osmium porphyrin complexes, Os(OEP)L_2 [OEP = octaethylporphin, L = py(pyridine) or NO], and PtOEP were investigated by picosecond laser spectroscopy with use of a double-beam, mode-locked Nd:glass system delivering 6-ps (fwhm) pulses at 527 nm with 1-2 mJ/pulse. Time-resolved excited-state spectra were recorded from the time of photoexcitation to 5 ns after photoexcitation. The initial excited state, S_1, decayed in ≤9 ps for the two osmium complexes and in ≤15 ps for the platinum porphyrin. A second excited state, T_1, lived for 1, 9, and >50 ns respectively for Os(OEP)$(py)_2$, Os(OEP)$(NO)_2$, and PtOEP. The Δ*A* spectra of the T_1 states of the osmium complexes were similar to those of previously reported (d_π,π^*) states for Os(OEP)$(py)_2$ and (π,π^*) states for Os(OEP)$(NO)_2$. This finding supports prior assignments of these states on the basis of expected axial and equatorial back-bonding of the osmium's d electrons. Additionally, a long-lived (τ > 5 ns) photochemical product (probably a result of ligand loss) was found in the case of Os(OEP)$(py)_2$.

Recent attempts to understand bonding and back-bonding relationships within biologically important iron porphyrins have been supported by studies of the related osmium porphyrins.[2] Osmium(II) porphyrins have d_{xy} and d_π (d_π = d_{xz},d_{yz}) orbitals of nearly the same energy as those of iron(II) porphyrins, but the Os(II) orbitals extend further into space, thus the π-back-bonding effects will be more pronounced for osmium than for iron porphyrins. The Fe(porphyrin)L_2 complexes are all labile in solution but Os(porphyrin)L_2 complexes are kinetically inert making reliable spectral and other physical data much easier to obtain for

[†] Brookhaven National Laboratory.
[‡] Concordia University.

(1) Visiting Research Associate from the Department of Chemistry, Concordia University.

(2) Buchler, J. W.; Kokisch, W.; Smith, P. D. *Struct. Bonding (Berlin)* **1978**, *34*, 79.

0002-7863/83/1505-4639$01.50/0

osmium porphyrins. Additionally, osmium(II) porphyrins should function as versatile electron donors, since the half-wave reduction potential for osmium(III) porphyrin/osmium(II) phorphyrin couples can be varied from +0.92 to −0.56 V vs. SCE simply by changing axial ligands.[2]

Rigidly linked, cofacial Mg and free-base porphyrins have been shown to be good models of the primary electron-transfer (ET) couple of photosystem II of green plants in that they produce stable ($\tau \sim 0.2$–1.3 ns) ET products from their $^1(\pi,\pi^*)$ excited states in less than 6 ps.[3,4] Similar studies on linked donor–acceptor couples containing an osmium porphyrin could explore the dependence of such light-driven ET reactions both on the redox potentials of the donors and acceptors and on the nature of the initial excited state.

The absorption and emission spectra of free-base porphyrins can be understood in terms of their highest occupied orbitals, $a_{2u}(\pi)$ and $a_{1u}(\pi)$, and of their lowest unoccupied orbitals, $e_g(\pi^*)$. When an $(nd)^6$ metal, such as Fe(II), Ru(II), or Os(II), is inserted into a porphyrin, the interplay between the metal's d electrons and the free-base porphyrin orbitals becomes important.[5-7] Axial ligands can either enhance or diminish metal–porphyrin interactions. With strong σ-donor ligands such as trimethylamine (NMe_3), pyridine (py), or trimethyl phosphite ($P(OMe)_3$), the filled d orbitals in osmium(II) porphyrins lie above the $a_{2u}(\pi)$ and $a_{1u}(\pi)$ porphyrin obitals.[8] This has two consequences. First, the d_π orbitals of Os(II) can back-bond with the empty $e_g(\pi^*)$ porphyrin orbitals. (The z axis is taken to be the direction of the axial ligands, perpendicular to the plane of the porphyrin ring.) The equatorial back-bonding interaction between the d_π and $e_g(\pi^*)$ orbitals raises the energy of the $e_g(\pi^*)$ orbitals relative to their location in a free-base porphyrin. Hence the allowed (π,π^*) absorptions in osmium(II) porphyrins with σ-donor ligands are hypsochromically shifted relative to their location in normal porphyrins. The second consequence of the filled d orbitals lying above the $a_{2u}(\pi)$ and $a_{1u}(\pi)$ orbitals is that forbidden charge-transfer (CT) transitions, $e_g(d_\pi) \rightarrow e_g(\pi^*)$, will lie below the allowed (π,π^*) states.

If the σ-donor ligands are replaced with π-acceptor ligands, the back-bonding of the d_π electrons shifts from equatorial to axial.[9] The ligands pyridine, carbon monoxide (CO), and nitrosonium (NO^+) are increasingly good π acceptors. As the back-bonding shifts from equatorial to axial, both the filled d_π and the empty $e_g(\pi^*)$ orbitals shift to lower energy. Experimentally the (π,π^*) absorptions bathochromically shift, the lowest excited state changes from (d_π,π^*) to (π,π^*) and the first oxidation potential becomes more positive, changing from metal to ring oxidation.

An earlier picosecond kinetic study[10] of the excited state spectra and relaxations of Os(porphyrin)L,L' complexes found both subnanosecond relaxation of an initial excited state (S_1) and nanosecond relaxation of a second excited state (T_1) in all cases. For porphyrins with (π,π^*) lowest energy excited states, S_1 and T_1 can be identified with spin quantum numbers $S = 0$ and $S = 1$, respectively. For porphyrins with (d_π,π^*) lowest energy excited states, spin is not expected to be a good quantum number. In these cases the initially formed excited state is expected to be $^1(\pi,\pi^*)$ and S_1 represents its relaxation products produced within ~ 1 ps. Presumably these are a subset of the (d_π,π^*) manifold of states. Therefore, the transition $S_1(d_\pi,\pi^*) \rightsquigarrow T_1(d_\pi,\pi^*)$ represents sublevel relaxation within the (d_π,π^*) manifold. An important result of the earlier study was that the excited-state spectra of the four Os(porphyrin)L,L' complexes studied supported previous assignments of the nature of the lowest energy excited state in each complex and thus also supported the equatorial–axial back-bonding model described above.[9] In particular the (d_π,π^*) excited states of $Os(OEP)[P(OMe)_3]_2$ (OEP = octaethylporphin) and Os(OEP)CO(py) absorbed at ~ 690 and ~ 715 nm while the (π,π^*) states of Os(OEP)NO(OMe) and $Os(OEP)O_2$ absorbed at ~ 605 and ~ 650 nm.[10] Also, as expected for four orbital transitions $[a_{2u}(\pi), a_{1u}(\pi) \rightarrow e_g(\pi^*)]$ in these excited states, each type of excited state ((π,π^*) or (d_π,π^*)) showed a bathochromic shift as the equatorial back-bonding decreased.

The overall objective of our current study is to test the generality of the above conclusions by examining other osmium porphyrin complexes with (d_π,π^*) and (π,π^*) lowest energy excited states respectively $Os(OEP)(py)_2$ and $Os(OEP)(NO)_2$. Additionally each of these porphyrins has unique features not found in other Os(porphyrin)L,L' complexes. For the dipyridine complex, extra absorption bands are found in the visible spectral region. These are attributed to allowed doubly excited states of the form $[e_g(d_\pi)]^3[a_{1u}(\pi),a_{2u}(\pi)]^3[e_g(\pi^*)]^2$ which couple by configuration interaction to the ring's singly excited states $[e_g(d_\pi)]^4[a_{1u}(\pi),a_{2u}(\pi)]^3[e_g(\pi^*)]^1$ to produce the observed "hyper" absorption spectrum. Also forbidden charge-transfer absorptions are found in the near infrared with the lowest one at 980 nm.[8] For the dinitrosyl complex, (π,π^*) states are lower in energy than (d_π,π^*) CT states. In other porphyrins where this is true, long-lived $^3(\pi,\pi^*)$ emission, ~ 100 μs at 77 K, is seen.[8,9] However, no emission is seen from this complex. Iterative Extended Hückel (IEH) calculations indicate that L_π^* orbitals may lie below the $e_g(\pi^*)$ orbitals in this case.[9] We wish to learn how the "extra" complications in the dipyridine and dinitrosyl osmium porphyrins affect the nature of the T_1 state, its lifetime, and its rate of formation from S_1.

Os(porphyrin)L,L' complexes with intermediate axial back-bonding such as Os(OEP)NO(OMe) are analogous to d^8 platinum porphyrins.[11] Both have filled d orbitals near, but below the $a_{2u}(\pi)$ and $a_{1u}(\pi)$ orbitals. This means that both types of porphyrins have (π,π^*) lowest energy excited states. In all such osmium porphyrins, $S_1(\pi,\pi^*) \rightsquigarrow T_1(\pi,\pi^*)$ relaxations are observed, yet this relaxation was not observed in an earlier study of platinum protoporphyrin IX dimethyl ester (PtPPDMe).[12] On the other hand, quasiline structure for the $^1(\pi,\pi^*)$ absorption band of Pt porphin in n-octane at 77 K implies that the $S_1(\pi,\pi^*)$ state should last ~ 1 ps.[13] Observation of this state during photoexcitation of a platinum porphyrin with a 6-ps pulse would unify our understanding of platinum and osmium porphyrins as well as support prior conclusions about metalloporphyrin lifetimes based on absorption line widths and fluorescence quantum yields. To this end we also measured the picosecond change-in-absorption (ΔA) spectra and kinetics of PtOEP in tetrahydrofuran (THF).

Experimental Methods

$Os(OEP)(py)_2$[8] and $Os(OEP)(NO)_2$[14] were synthesized according to published procedures. Chromatographically purified PtOEP was purchased from Mid-Century Chemicals. Its UV–vis spectrum agreed with literature values[15,16] and it was used without further purification. Fisher Scientific Co. certified reagent grade tetrahydrofuran was used without further purification.

The picosecond absorbance measurements were made on a double-beam, mode-locked Nd:glass laser system employing a SIT-vidicon detector.[4,17] ΔA spectra at a designated time after excitation at 527 nm

(3) Netzel, T. L.; Kroger, P.; Chang, C.-K.; Fujita, I.; Fajer, J. *Chem. Phys. Lett.* **1979**, *67*, 223.
(4) Netzel, T. L.; Bergkamp, M. A.; Chang, C.-K. *J. Am. Chem. Soc.* **1982**, *104*, 1952.
(5) Buchler, J. W. "Porphyrins and Metalloporphyrins"; Smith, K. M., Ed.; Elsevier: Amsterdam, 1975; Chapter 5, p 157.
(6) Buchler, J. W. "The Porphyrins"; Dolphin, D., Ed.; Academic Press: New York, 1978; Vol. I, Part A, Chapter 10, p 389.
(7) Gouterman, M., in ref 5, Vol. III, Part A, Chapter 1, p 1.
(8) Antipas, A.; Buchler, J. W.; Gouterman, M.; Smith, P. D. *J. Am. Chem. Soc.* **1978**, *100*, 3015.
(9) Antipas, A.; Buchler, J. W.; Gouterman, M.; Smith, P. D. *J. Am. Chem. Soc.* **1980**, *102*, 198.
(10) Serpone, N.; Netzel, T. L.; Gouterman, M. *J. Am. Chem. Soc.* **1982**, *104*, 246.
(11) Ake, R. L.; Gouterman, M. *Theor. Chem. Acta* **1970**, *17*, 408.
(12) Kobayashi, T.; Straub, K. D.; Rentzepis, P. M. *Photochem. Photobiol.* **1979**, *29*, 925.
(13) Callis, J. B.; Gouterman, M.; Jones, Y. M.; Henderson, B. H. *J. Mol. Spectrosc.* **1971**, *39*, 410.
(14) Buchler, J. W.; Smith, P. D. *Chem. Ber.* **1976**, *109*, 1465.
(15) Smith, K. M., Ed. "Porphyrins and Metalloporphyrins"; Elsevier: Amsterdam, 1975.
(16) Eastwood, D.; Gouterman, M. *J. Mol. Spectrosc.* **1970**, *35*, 359.

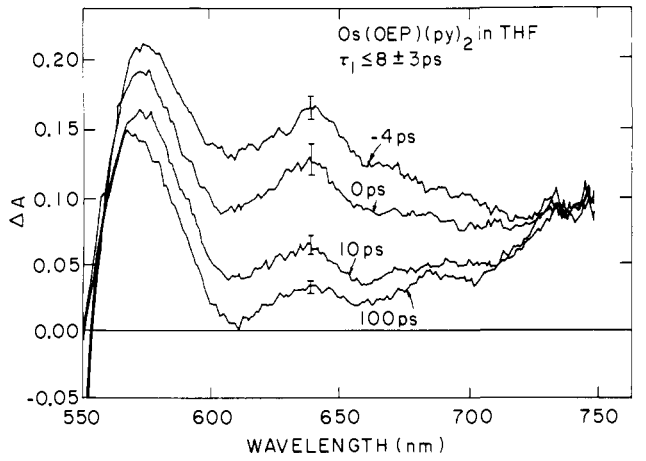

Figure 1. Change-in-absorbance (ΔA) spectra for $Os(OEP)(py)_2$ in tetrahydrofuran (THF) at the indicated optical delay times after photoexcitation. The indicated delay times refer to 750 nm and must be ajdusted for time dispersion for use at other wavelengths. (See the text for further details.)

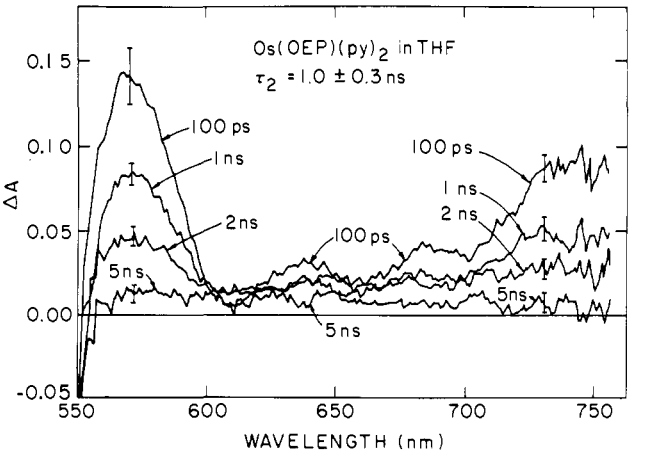

Figure 2. Change-in-absorbance (ΔA) spectra for $Os(OEP)(py)_2$ in THF in the 100-ps to 5-ns time interval.

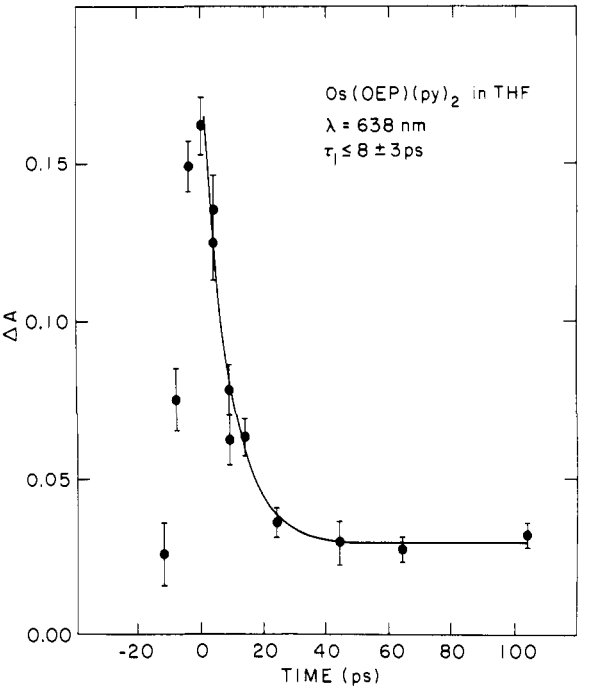

Figure 3. Kinetic plot of ΔA vs. time at 638 nm for $Os(OEP)(py)_2$ in THF. The decay kinetics are pulse determined and not a measure of the S_1 state's true lifetime. The solid line is an exponential fit to the data with an 8-ps decay lifetime.

with a 6-ps (fwhm) laser pulse are the average of 15–20 pairs of laser shots. One laser shot of a pair recorded the double-beam ratios at 250 wavelengths in the 500–800-nm range when the sample was not excited. The other shot repeated the measurements when the sample was excited. The log of the ratio of these double-beam ratios yielded the reported ΔA values. The standard deviation of the mean ΔA value is the calculated error of the measurement and is indicated in the figures. The data points shown in the kinetic plots of ΔA vs. time are the same data as presented in the ΔA vs. wavelength plots. Thus each time-point in the kinetic plots is also the average ΔA from 15–20 pairs of laser shots.

A 0.25-m double monochromator (DMC) in the subtractive dispersion mode was placed after the sample but before the final spectrograph to reject stray excitation light. It was equipped with two 150-grooves/mm gratings and a 10-mm intermediate slit which passed about 300 nm of spectral information. However, the sharp drop in transmitted light at the edges of the band-pass region truncated the ΔA values of 0 at these edges.

The white probe light was generated by focusing 1054-nm laser light into a 5-cm cell containing D_2O. The duration of the weak probe pulse was 8 ps (fwhm). The 6-ps excitation pulse at 527 nm contained 1–2 mJ of energy. The Laser Precision energy meter coupled to a sample-and-hold circuit and a PDP 11/03-controlled A-to-D converter ensured that data from pulses outside this energy interval were rejected. After passing through the DMC, the white probe light was dispersed by a 150-grooves/mm grating in a second 0.25-m monochromator. The 0.5-mm wide entrance slit yielded a resolution of 12 nm. The response time of the Nd:glass laser system was 9 ± 3 ps, due to the convolution of the excitation and probe pulses. The measurement times in the spectral and kinetic plots refer to optical delay times determined by the position of a translation state in the excitation beam. The error in locating the translation stage corresponded to an error in measurement time of less than 0.1 ps and therefore was negligible in this study.

The effects of time dispersion in the white probe pulse are important for the S_1 excited states in these complexes because of their very short lifetimes (<25 ps). Light of shorter wavelength travels more slowly in dense media such as water and glass than does light of longer wavelength. In other words if light at 775 nm is coincident in the sample with the excitation pulse, light at 600 nm will not get to the sample for several more picoseconds. In our apparatus there is about 1 ps of delay for each 35 nm of spectral increment in the 550–775-nm region. These delays are not significant for optical transients with lifetimes >25 ps. We have adopted the proceure in the figures of specifying the time of arrival of the longest wavelength light at the sample cell relative to the excitation pulse. Negative time means that the longest wavelength light arrived before or during the excitation pulse, while positive time means that it arrived after the excitation pulse. In order to calculate the arrival time of any other wavelength, the delay at that wavelength must be added to the longest wavelength's arrival time. For example a ΔA spectrum probing the 775-nm region at −4 ps is probing the 600-nm region +1 ps after excitation.

All samples were either degassed by repeated freeze–pump–thaw cycles and kept in flame-sealed seals or degassed by Argon bubbling and kept in serum capped cells. The optical path length of the cells was 2 mm and the sample concentrations were 2.5×10^{-4}, 1.7×10^{-4}, and 1.0×10^{-4} M respectively for $Os(OEP)(py)_2$, $Os(OEP)(NO)_2$, and PtOEP.

Results

(a) $Os(OEP)(py)_2$. The dipyridine complex has extensive equatorial back-bonding [$d_\pi + e_g(\pi^*)$] as evidenced by its hypsochromically shifted Q band [$^1(\pi,\pi^*)$ absorption] at 510 nm. The visible absorption spectrum is also of a "hyper" type in that extra allowed bands due to doubly excited states of the form $[e_g(d_\pi)]^3[a_{1u}(\pi),a_{2u}(\pi)]^3[e_g(\pi^*)]^2$ are seen as low as 600 nm (see above). In the near infrared, forbidden $d_\pi \rightarrow e_g(\pi^*)$ CT transitions are found at 650, 720, 850, and 980 nm.[8]

Figures 1 and 2 show the ΔA spectra for $Os(OEP)(py)_2$ in THF from the time of photoexcitation to 5 ns after photoexcitation. The slight dips in the ΔA spectra around 600, 650, and 720 nm correspond to regions of ground-state absorbance. The band shape of the T_1 state, strong ΔA increases in the 550–600- and 700–750-nm regions separated by a valley of small ΔA increase, is very similar to the band shapes of the T_1 states of $Os(OEP)[P(OMe)_3]_2$ and $Os(OEP)CO(py)$.[10]

(17) Creutz, C.; Chou, M.; Netzel, T. L.; Okumura, M.; Sutin, N. *J. Am. Chem. Soc.* **1980**, *102*, 1309.

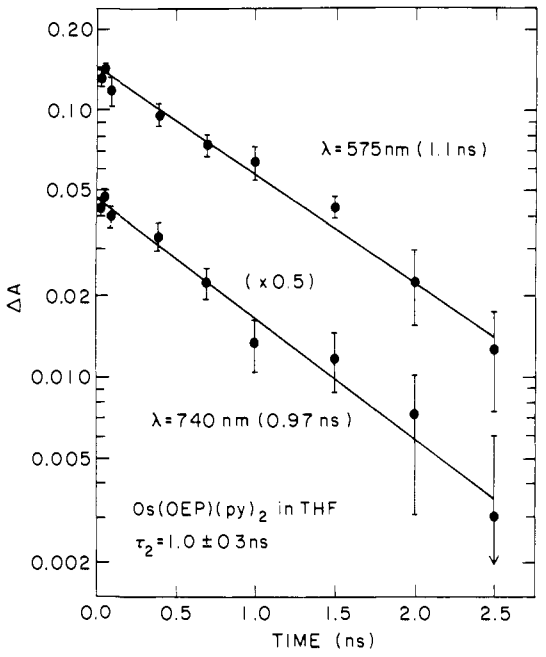

Figure 4. Kinetic plots of ΔA vs. time at the indicated wavelengths for the decay of the T_1 state of $Os(OEP)(py)_2$ in THF. The solid lines are least-squares fits to the data with the first-order decay lifetimes shown in parentheses.

Figure 3 is a kinetic plot of ΔA vs. time for the 638-nm region immediately before and after photoexcitation. The decay of this ΔA increase mirrors its rise and shows that the S_1 state is so short lived ($\leq$9 ps) that it is only observed during photoexcitation. The solid line is an exponential fit to the data and respresents the minimum response time of our laser system. A similar pulse-determined lifetime was reported earlier for the $S_1 \rightsquigarrow T_1$ relaxation in $Os(OEP)[P(OMe)_3]_2$.[10] Figure 4 presents kinetic plots of ΔA vs. time data for the decay of the T_1 state at 575 and 740 nm. The measured lifetime is 1.0 ± 0.3 ns, which is the shortest (d_π,π^*) lifetime yet observed in an osmium porphyrin.

Inspection of the 5-ns spectrum in Figure 2 shows that a ΔA increase persists even at this long time. Since less than 1% of the T_1 state's signal is present at this time, it cannot be due to T_1. Additional measurements in the 4–5-ns range confirmed the existence of this optical transient. It is unlikely that this signal is due to a long-lived excited state of $Os(OEP)(py)_2$, rather it probably represents pyridine loss. To test this possibility we studied this complex in THF with 50% by volume pyridine. In this case the optical transient at 5 ns was nearly completely eliminated. A solution of $Os(OEP)(py)_2$ with 10% pyridine in THF gave results intermediate between those of solutions of the complex with 0 and 50% pyridine in THF.

It should be pointed out that solutions of $Os(OEP)(py)_2$ in THF were quite stable and no net photochemistry was observable on a seconds time scale. Whether or not axial ligand loss due to photoexcitation occurs in other osmium porphyrin complexes (especially those with $T_1(d_\pi,\pi^*)$ states) cannot be directly determined as the longest time our laser system can measure is 5 ns and all other osmium porphyrin complexes have T_1 lifetimes in the 6–16-ns range.[10] Only in $Os(OEP)(py)_2$ with a 1-ns T_1 state could we directly search for photochemical products after the decay of excited states.

Indirect evidence for axial ligand release due to photoexcitation exists for the hypso porphyrin $Os(OEP)[P(OMe)_3]_2$. (Both $Os(OEP)[P(OMe)_3]_2$ and $Os(OEP)(py)_2$ have $T_1(d_\pi,\pi^*)$ lowest energy excited states and show no detectable emission, even at 77 K.) The trimethyl phosphite complex was found to react photochemically in chlorinated solvents and addition of excess $P(OMe)_3$ inhibited the reaction.[18] The final product was identified as $Os(OEP)Cl_2$ on the basis of its characteristic Os(IV) spectrum and the first steps of the probable reaction mechanism were proposed to be light-activated axial ligand release followed by solvent attack on the five-coordinate porphyrin.

(18) Serpone, N.; Jamieson, M.; Netzel, T. L. *J. Photochem.* **1981**, *15*, 295.

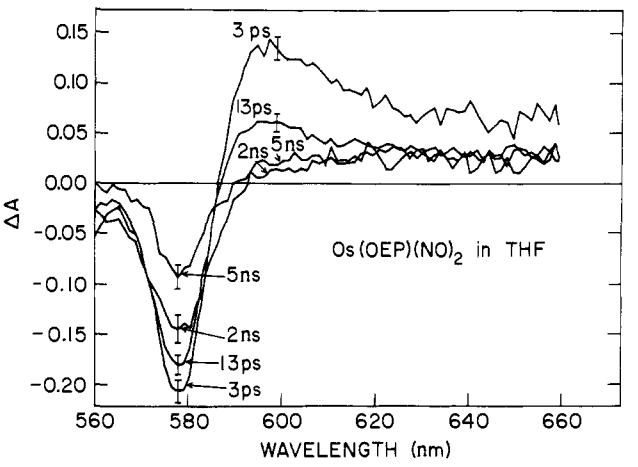

Figure 5. Change-in-absorbance (ΔA) spectra for $Os(OEP)(NO)_2$ in THF at the indicated optical delay times after photoexcitation. The indicated delay times refer to 660 nm. (See Figure 1 and the text for time dispersion corrections for other wavelengths.)

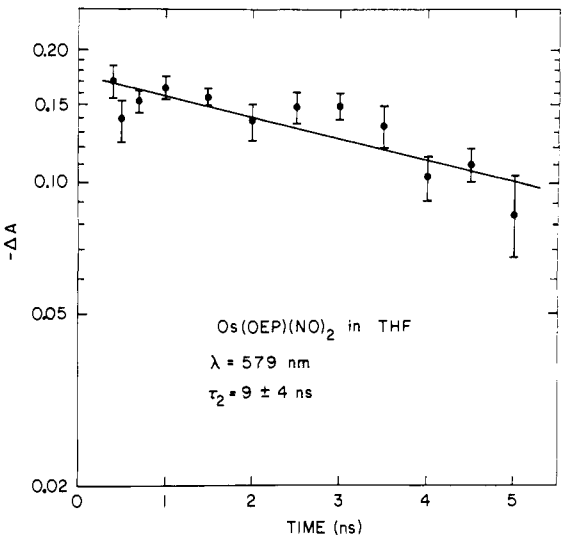

Figure 6. Kinetic plot of ΔA versus time for the decay of the T_1 state of $Os(OEP)(NO)_2$ in THF. The solid line is a least-squares fit to the data with a first-order decay lifetime of 9 ns.

(b) $Os(OEP)(NO)_2$. The dinitrosyl complex has much more axial back-bonding than $Os(OEP)(py)_2$. Its Q-band absorption is at 576 nm and cannot be classified as hypso.[9] It is closely related to Os(OEP)NO(F) and Os(OEP)NO(OMe) with Q(0,0) bands at 567 nm.[9] Both of these latter complexes have $T_1(\pi,\pi^*)$ lowest excited states that show structured emissions with lifetimes of over 100 μs at 77 K.[8,9] The absorption spectra of all three nitrosyl porphyrin complexes are hyper due to (π,L_π^*) absorptions in the 330–350-nm region. The presence of L_π^* orbitals above the $e_g(\pi^*)$ orbitals tends to red shift both the Soret and Q bands of these porphyrins. However the (π,L_π^*) band is lowest in energy and most intense for $Os(OEP)(NO)_2$. Additionally, its orbital structure is calculated (IEH method) to be more complicated than that of the other two nitrosyl porphyrin complexes.[9] A filled π orbital on NO^- is close in energy to the $a_{2u}(\pi)$ orbital and several unoccupied ligand π and π^* orbitals could be located close to and below the $e_g(\pi^*)$ orbitals. In fact $Os(OEP)(NO)_2$ shows no emission, even at 77 K. Low-energy transitions among the filled and unoccupied ligand orbitals have been proposed as reponsible for this.[9]

Figure 5 presents ΔA vs. wavelength plots for $Os(OEP)(NO)_2$ in THF at various times after excitation. The lifetime of the

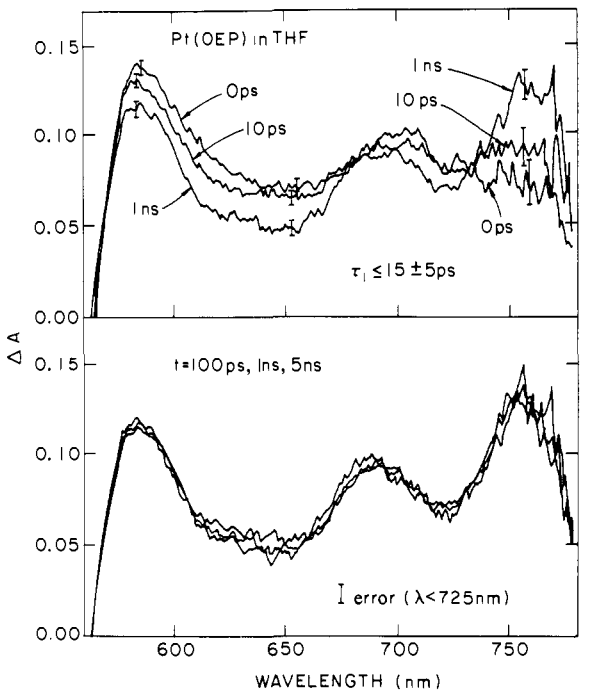

Figure 7. Change-in-absorbance (ΔA) spectra for PtOEP in THF at the indicated optical delay times after photoexcitation. The indicated delay times refer to 775 nm. (See Figure 1 and the text for time dispersion corrections for other wavelengths.)

$S_1(\pi,\pi^*)$ state is completely pulse determined, ≤9 ps. Figure 6 is a ΔA vs. time plot of the decay of the T_1 state in the ground-state bleaching region at 579 nm. Its lifetime is 9 ± 4 ns.

(c) PtOEP. Figure 7 presents ΔA vs. wavelength plots for PtOEP in THF at various times after excitation. Two transients are seen with the first, $S_1(\pi,\pi^*)$ slightly more strongly absorbing than the second, $T_1(\pi,\pi^*)$, in the short-wavelength region of Figure 7 and the reverse true in the long-wavelength region. Also, both states absorb similarly in the 680–720-nm region. We have previously found the $S_1(\pi,\pi^*)$ state of free-base octaethylporphin (H_2OEP) to absorb more strongly in the short-wavelength region above 500 nm than its $T_1(\pi,\pi^*)$ state and the reverse true in the long-wavelength region below 800 nm.[19] Perhaps not surprisingly the ΔA spectra in Figures 1, 5, and 7 are all dissimilar. The first are for (d_π,π^*) states, the second for (π,π^*) states with higher lying L_π^* orbitals present, and the third for (π,π^*) states without higher energy L_π^* orbitals, but there is some similarity between ΔA spectra for two octaethylporphyrins without axial ligands, H_2OEP and PtOEP.

The bottom panel of Figure 7 shows that the T_1 state of PtOEP does not decay during our 5-ns observation time ($\tau > 50$ ns). This agress with a room-temperature lifetime of 63 μs for the T_1 state of Pt(etio) [etio = etioporphyrin I].[13] Figure 8 presents a plot of ΔA vs. time for the $S_1 \rightsquigarrow T_1$ relaxation in PtOEP at 585 nm. The two solid curves are exponential fits to the data with lifetimes of 9 and 13 ps, as indicated. Because of the uncertainty in the asymptote of this relaxation, lifetimes as large as 18 ps also fit the data reasonably well. The major difficulty is that the change in ΔA between the S_1 and T_1 states is quite small, ~0.04. (An earlier study of PtPPDME at 480 and 550 nm by Kobayashi et at.[12] did not observe the $S_1 \rightsquigarrow T_1$ relaxation. Perhaps the change in ΔA on going from S_1 to T_1 is nearly zero for PtPPDMe at these wavelengths.) The data in Figure 8 yield an apparent lifetime of 15 ± 5 ps. Clearly this is an upper limit to the real lifetime of S_1. In fact, we cannot rule out a true S_1 lifetime as short as 1 ps, which would yield instrument response limited decay kinetics. For S_1 lifetimes much shorter than 1 ps, we probably will not see any evidence of the S_1 state unless its difference in molar extinction coefficient ($\Delta\epsilon$) between S_1 and S_0 were much larger than that between T_1 and S_0. This is unlikely for (π,π^*) excited states in porphyrins without axial ligands.

(19) Netzel, T. L.; Fujita, I., unpublished observation.

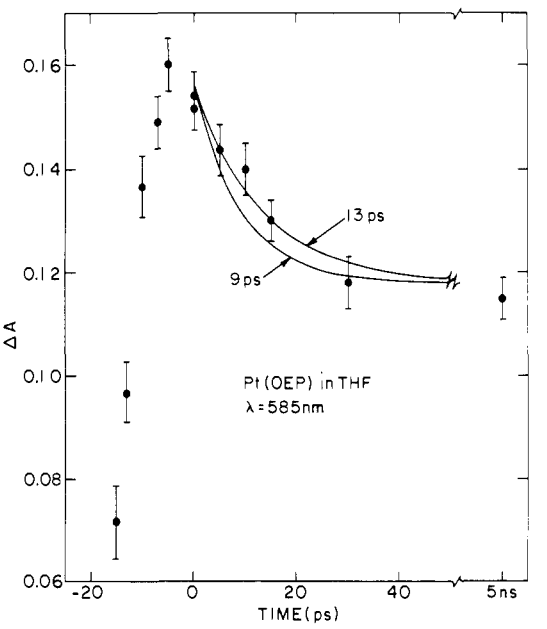

Figure 8. Kinetic plot of ΔA vs. time for the formation and decay of the $S_1(\pi,\pi^*)$ state of PtOEP in THF at 585 nm. The solid lines are fits to the data for first-order decays with the indicated lifetimes.

Discussion

An earlier study[13] on platinum porphyrins found that the fluorescence quantum yield of platinum porphin was less than 2×10^{-5}. Since the radiative lifetime of its S_1 state is most likely 60–70 ns,[20,21] its lifetime (τ) should be less than 1.5 ps. A lower limit to its lifetime was inferred from quasiline spectra of the Q(0,0) band of platinum porphin in *n*-octane at 77 K.[13] Because

$$\tau\Delta\nu \geq (2\pi c)^{-1} \qquad (1)$$

where $\Delta\nu$ is the width at half-maximum of the absorption quasilines and c is the speed of light, an approximately 8-cm^{-1} lifetime broadening of the Q(0,0) quasilines of platinum porphin implies that τ should be greater than or equal to 0.7 ps. Thus platinum porphyrins should have $^1(\pi,\pi^*)$ states that live for ~1 ps, yet an earlier study of PtPPDME with 6-ps excitation pulses did not observe the S_1 state even during photoexcitation.[12] The observation in this work of the S_1 state of PtOEP is consistent with expectations that it lives for ~1 ps and shows that the observation of $^1(\pi,\pi^*)$ states in metalloporphyrins with 5d electrons is not unique to osmium porphyrin complexes.

While platinum(II) porphyrins have eight d electrons, they have strong similarities to d^6 osmium(II) porphyrins with intermediate axial and equatorial back-bonding, e.g., Os(OEP)NO(OMe) and Os(OEP)$(NO)_2$. In both cases the filled d orbitals lie below $a_{2u}(\pi)$ and $a_{1u}(\pi)$ porphyrin orbitals so that (π,π^*) transitions are at lower energy than (d,π^*) transitions.[9,11,16] However, platinum porphyrins have no axial ligands so that perturbations of the $e_g(\pi^*)$ orbitals by nearby L_π^* orbitals are absent. Thus differences between osmium porphyrins with $T_1(\pi,\pi^*)$ states and platinum porphyrins are probably ascribable to axial ligand influences.

Table I lists a variety of excited-state properties and lifetimes for both Os(OEP)L,L′ and platinum porphyrins. The room-temperature lifetimes of the S_1 states of these compounds are all less than 100 ps with most less than 15 ps. Since this result is insensitive to the type of axial ligands (and therefore to the degree of axial or equatorial back-bonding) in osmium porphyrins and

(20) A lifetime obtained from integration of the absorption spectra of some other metalloporphyrins.[21]

(21) Seybold, P. G.; Gouterman, M. *J. Mol. Spectrosc.* **1969**, *31*, 1.

Table I. Excited-State Properties of Osmium and Platinum Porphyrins[a]

compound	Q(0,0)[b] (nm)	$T_1(0,0)$[c] (nm)	ΔE_{Q-T}[d] (cm^{-1})	τ_S(295 K)[e] (ps)	τ_T(295 K)[f] (ns)	τ_T(77 K)[g] (μs)	Q_T(77 K)[h]
A. Porphyrins with (d_π,π^*) States below (π,π^*) States							
Os(OEP)$(py)_2$	510[i]	no emission		≤ 9	1		$<10^{-4}$[i]
Os(OEP)$[P(OMe)_3]_2$	522[i]	no emission		≤ 9[j]	6[j]		$<10^{-4}$[i]
Os(OEP)CO(py)	537[i]	720[i]	4730	~50[j]	16[j]	<6[i]	6×10^{-4}[i]
B. Porphyrins with (π,π^*) States below (d_π,π^*) States							
Pt(etio)	536[k]	641[k]	3056	≤ 15[l]	63 μs[m,n]	125[m]	0.9[k]
Os(OEP)NO(OMe)	568[i]	688[i]	3070	~36[j]	6[j]	116/135[i]	3×10^{-3}[i]
Os(OEP)$(NO)_2$	576[o]	no emission		≤ 9	9		$<3 \times 10^{-4}$[i]
Os(OEP)O_2	594[i]	729[i]	3120	≤ 13[j]	6[j]	103/21[o]	$\sim 5 \times 10^{-3}$[i]

[a] The following abbreviations are used: OEP = octaethylporphin, py = pyridine, $P(OMe)_3$ = trimethyl phosphite, etio = etioporphyrin I, OMe = methoxide, O_2 = dioxo. [b] Wavelength of the lowest energy $^1(\pi,\pi^*)$ absorption band. [c] Origin of phosphorescence. [d] Energy gap between $Q(0,0)$ absorption and $T_1(0,0)$ emission. [e] S_1-state lifetime at 295 K. [f] T_1-state lifetime at 295 K. [g] T_1-state lifetime at 77 K measured by emission decay. [h] T_1-state emission quantum yield at 77 K. [i] Reference 8. [j] Reference 10. [k] Reference 16. [l] Lifetime actually measured for PtOEP which should be very much like Pt(etio). [m] Reference 13. [n] This work shows that the room-temperature lifetime of the $T_1(\pi,\pi^*)$ state of PtOEP is >50 ns. [o] Reference 9.

even to the absence of axial ligands in platinum porphyrins, it is fair to conclude that the rapid $S_1 \rightsquigarrow T_1$ relaxations in these compounds are almost entirely governed by their central metal atoms.

The ΔA spectra for the T_1 state of Os(OEP)$(py)_2$, see Figure 2, are very similar to those of the T_1 states of Os(OEP)$[P(OMe)_3]_2$ and Os(OEP)CO(py).[10] Both of these latter complexes have hypsochromically shifted Q bands, respectively 522 and 537 nm, and their T_1 states have been assigned as (d_π,π^*).[8,9] Thus the T_1 spectra ($t > 20$ ps) in Figures 1 and 2 support the back-bonding model's prediction of (d_π,π^*) states at lower energy than (π,π^*) states for Os(OEP)$(py)_2$.[9] This also agrees with the assignments of the near-infrared bands as forbidden $d_\pi \rightarrow e_g(\pi^*)$ transitions.[8]

The ΔA spectra for the S_1 and T_1 states of Os(OEP)$(NO)_2$, see Figure 5, look remarkably like those found for the $S_1(\pi,\pi^*)$ and $T_1(\pi,\pi^*)$ states of Os(OEP)NO(OMe) and Os(OEP)O_2.[10] Also the bathochromic shift of (π,π^*) excited-state absorptions noted earlier is present and parallels that of the Q(0,0) ground-state absorptions: ~595, ~605, and ~650 nm for excited-state maxima and 568, 576, and 594 nm for Q(0,0) respectively for Os(OEP)NO(OMe), Os(OEP)$(NO)_2$, and Os(OEP)O_2. Thus the picosecond ΔA spectra support assigning the T_1 state of Os(OEP)$(NO)_2$ as $^3(\pi,\pi^*)$. Also, its room-temperature lifetime is comparable to the 6-ns $T_1(\pi,\pi^*)$ lifetime at room temperature of both Os(OEP)NO(OMe) and Os(OEP)O_2.[10]

Part A of Table I shows that the T_1-state lifetimes at room temperature vary inversely with the hypsochromic shift of the Q(0,0) band for osmium porphyrins with (d_π,π^*) lowest energy excited states. Most likely this reflects an increasing energy gap between $T_1(d_\pi,\pi^*)$ and S_0 as equatorial back-bonding decreases and axial back-bonding increases. A similar trend is not apparent in part B of Table I for osmium prophyrins with $T_1(\pi,\pi^*)$ states.

Table I also lists the available data on the temperature dependence of the T_1 states of osmium and platinum porphyrins. The $T_1(\pi,\pi^*)$ states of platinum porphyrins exhibit very little lifetime increase (~2×) on going from 295 to 77 K. The same is apparently true for the $T_1(d_\pi,\pi^*)$ state of Os(OEP)CO(py) although only an upper limit is available for its lifetime at 77 K. In contrast, very large temperature effects (>10^4) are found for the $T_1(\pi,\pi^*)$ states of Os(OEP)NO(OMe) and Os(OEP)O_2. Remarkably, their room-temperature lifetimes are similar to those of (d_π,π^*) states while their 77 K lifetimes are like that of the $^3(\pi,\pi^*)$ state of Pt(etio). These facts suggest that at room temperature they may be deactivated by thermal population of higher energy (d_π,π^*) states. Additionally their low phosphorescence quantum yields relative to that of Pt(etio) may indicate that their lifetimes and emission yields will substantially lengthen on going to lower temperatures.

Presumably the T_1 state of Os(OEP)(NO_2) is relatively short lived (<6 μs) at 77 K, since no phosphorescence is detectable. Both the Soret and Q bands of this compound are bathochromically shifted due to nearby (π,L_π^*) states.[9] Additionally there may be low-energy transitions between filled and unoccupied ligand orbitals below the $T_1(\pi,\pi^*)$ state.[9] If lower energy transitions are responsible for the decay of T_1, measurements at lower temperatures probably will not find substantially increased T_1 lifetimes. However, if T_1 is being depopulated at 77 K by a nearby, but higher energy, $^3(\pi,L_\pi^*)$ states, long lifetimes at low temperatures are possible.

Summary

The ΔA spectra of the T_1 states of Os(OEP)$(py)_2$ and Os(OEP)$(NO)_2$ were found to have characteristic (d_π,π^*) and (π,π^*) features, respectively. This result extends the generality of prior picosecond studies[10] of osmium porphyrins and confirms the theoretical predictions[8,9] of axial-ligand influences on d_π back-bonding interactions. Additionally the ultrafast (>10^{10} s^{-1}) S_1 to T_1 excited-state relaxations were found to be generally characteristic of osmium(II) and platinum(II) porphyrins and not significantly affected by the presence or absence of axial ligands.

The mixing of doubly excited states with singly excited ones in the visible region of the spectrum of Os(OEP)$(py)_2$ does not appear to have significantly influenced the S_1 and T_1 excited-state relaxations of this complex. However, its high-lying d_π levels do produce a small $T_1(d_\pi,\pi^*)$ to S_0 energy gap and the shortest T_1 excited-state lifetime yet observed for an osmium porphyrin.

The absence of detectable phosphorescence of Os(OEP)$(NO)_2$ at 77 K may be due to (π,L_π^*) transitions below the T_1 states (as previously suggested[9]), but the room-temperature lifetime (9 ns) of the T_1 state is much and same as that of Os(EOP)NO(OMe) and Os(OEP)O_2 (both 6 ns). Since all three of these porphyrins have very similar ΔA spectra for their T_1 states, they are apparently all (π,π^*) in character (as expected from back-bonding predictions). Thus it is possible that even at 77 K the $T_1(\pi,\pi^*)$ state of Os(OEP)$(NO)_2$ is being thermally deactivated by a nearby, but higher energy, $^3(\pi,L_\pi^*)$ state. Low-temperature emission and absorption studies may be able to determine which of the above possible situations actually obtains.

Low-energy transitions below the $T_1(\pi,\pi^*)$ states of Os(OEP)NO(OMe) and Os(OEP)O_2 are unlikely and indeed these states show structured phosphorescence with lifetime of ~100 μs at 77 K.[8,9] In contrast, their room-temperature lifetimes are both 6 ns.[9] The lifetime of the $T_1(\pi,\pi^*)$ state of Pt(etio) varies by only a factor of 2 over this same temperature range: 63 μs at 295 K and 125 μs at 77 K.[13] These observations suggest that thermal deactivation of T_1 by a higher energy (d_π,π^*) level may be an important decay route at room temperature. Lifetime measurements at lower temperatures may find even longer T_1 lifetimes and larger phosphorescence quantum yields.

Acknowledgment. We would like to thank Mr. G. Cousineau for his assistance in the synthesis of the osmium porphyrin complexes. Research carried out at Concordia University was supported by the Natural Sciences and Engineering Research Council

(NSERC) of Canada (Ottawa), the Formation de Chercheurs et d'Action Concertée (Quebec), and the North Atlantic Treaty Organization (No. 046.81); work at Brookhaven National Laboratory was done under contract with the U.S. Department of Energy and supported by its Office of Basic Energy Sciences. N.S. is grateful to NSERC (Ottawa) for a generous grant for the Canadian Picosecond Laser Laboratory at Concordia University.

Registry No. $Os(OEP)(py)_2$, 51286-87-4; $Os(OEP)(NO)_2$, 59296-75-2; PtOEP, 31248-39-2.

Ligand Design and Metal-Ion Recognition. Interaction of Nickel(II) with 17- to 19-Membered Macrocycles Containing O_2N_3 and O_3N_2 Donor Sets and the X-ray Structure of the Parent 17-Membered Macrocyclic Ligand

Kenneth R. Adam,[1a] Anthony J. Leong,[1a] Leonard F. Lindoy,*[1a] Hyacinth C. Lip,[1a] Brian W. Skelton,[1b] and Allan H. White[1b]

Contribution from the Department of Chemistry and Biochemistry, James Cook University, Queensland, 4811 Australia, and Chemistry Department, University of Western Australia, Nedlands, Western Australia, 6009 Australia. *Received October 12, 1982*

Abstract: A range of 17-19-membered macrocycles incorporating O_2N_3 and O_3N_2 donor sets has been synthesized and their interaction with nickel(II) studied. The X-ray structure of the parent 17-membered O_2N_3 ring indicates that the macrocyclic hole size is too large to enable simultaneous coordination of all donor atoms to nickel unless ligand folding occurs. An investigation of a selection of the nickel complexes in the solid state and in solution has been performed, and in all cases the results are consistent with the presence of either octahedral or pseudo-octahedral coordination geometries. In solution, the unsubstituted 17- and 18-membered O_2N_3 rings appear to adopt a configuration about nickel in which two oxygens and two nitrogens occupy equatorial positions while the remaining nitrogen coordinates at an axial site. The remaining axial position is occupied by a halide ion. In contrast, apparently as a consequence of steric crowding in the portion of the ligand backbone incorporating the three nitrogen donors, each of the 19-membered ring complexes are found to adopt a structure different from that of the above complexes. A similar structural "dislocation" can be induced by introduction of two methyl substituents onto the N_3-containing backbone of the unsubstituted 17-membered ring complex. The effects of such structural dislocations are most readily apparent in the stability constant variations observed across this series of complexes. The complexes postulated to undergo such dislocations give stability constants that are 10^3-10^5 lower than the remaining complexes. A comparison of the stability constants for the nickel complexes with those for the corresponding cobalt(II) complexes indicates that both series have similar "dislocation" patterns. In contrast, the complexes of copper(II) (for which the evidence suggests noncoordination of one or both ether oxygens in some complexes) exhibit a different stability pattern. The different behavior for copper, coupled with a knowledge of where dislocations occur for nickel and cobalt, makes possible the selection of reagents showing enhanced discrimination for copper over these other ions. More important, the study serves to illustrate the manner in which minor changes in macrocyclic ligand structure can be used to control alternate modes of ligand coordination—a process that can contribute to metal-ion recognition by organic substrates.

Introduction

An understanding of the factors underlying metal-ion recognition by organic substrates has wide-ranging ramifications for many areas of both chemistry and biochemistry. We have previously published accounts of the interaction of a number of transition- and post-transition-metal ions with a range of oxygen–nitrogen and sulfur–nitrogen donor macrocycles;[2-5] a principal aim of these studies has been to search for metal–ion discrimination and to understand the nature of such discrimination when it does occur. Mixed-donor complexes have proved especially suitable for such studies since they do not exhibit the large kinetic and thermodynamic stabilities that in some cases have made the solution study of related all-nitrogen donor systems somewhat difficult.[6]

Apart from the usual parameters influencing the affinities of open-chain ligands for particular ions (namely, variation of structural factors, donor-atom type, etc.), cyclic ligands can be further "tuned" by adjusting the macrocyclic hole size until an optimum fit for the metal ion of interest is achieved. Such use of macrocyclic hole-size variation to control the thermodynamic stabilities of metal complexes is of considerable current interest, and many studies of this type involving cyclic polyether ligand and non-transition-metal ions have been reported.[7] However, similar studies directed at achieving metal-ion specificity for particular transition ions have received less attention. In a previous investigation of this latter type, comparisons of the kinetic and thermodynamic stabilities of the nickel complexes of the 14-17-

(1) (a) James Cook University. (b) University of Western Australia.
(2) Armstrong, L. G.; Grimsley, P. G.; Lindoy, L. F.; Lip, H. C.; Norris, V. A.; Smith, R. J. *Inorg. Chem.* **1978**, *17*, 2350–2352. Ekstrom, A.; Lindoy, L. F.; Lip, H. C.; Smith, R. J.; Goodwin, H. J.; McPartlin, M.; Tasker, P. A. *J. Chem. Soc., Dalton Trans.* **1979**, 1027–1031. Adam, K. R.; Anderegg, G.; Lindoy, L. F.; Lip, H. C.; McPartlin, M.; Rea, J. H.; Smith, R. J.; Tasker, P. A. *Inorg. Chem.* **1980**, *19*, 2956–2964. Lindoy, L. F.; Lip, H. C.; Rea, J. H.; Smith, R. J.; Henrick, K.; McPartlin, M.; Tasker, P. A. *Ibid.* **1980**, *19*, 3360–3365. Lindoy, L. F.; Smith, R. J. *Ibid.* **1981**, *20*, 1314–1316.
(3) Anderegg, G.; Ekstrom, A.; Lindoy, L. F.; Smith, R. J. *J. Am. Chem. Soc.* **1980**, *102*, 2670–2674.
(4) Ekstrom, A.; Lindoy, L. F.; Smith, R. J. *Inorg. Chem.* **1980**, *19*, 724–727.
(5) Adam, K. R.; Lindoy, L. F.; Lip, H. C.; Rea, J. H.; Skelton, B. W.; White, A. H. *J. Chem. Soc., Dalton Trans.* **1981**, 74–79.
(6) Anichini, A.; Fabbrizzi, L.; Paoletti, P.; Clay, R. M. *J. Chem. Soc., Dalton Trans.* **1978**, 577–583. Hinz, F. P.; Margerum, D. W. *Inorg. Chem.* **1974**, *13*, 2941–2949. Tabushi, I.; Fujiyoshi, M. *Tetrahedron Lett.* **1978**, 2157–2160.
(7) Lehn, J. M. *Struct. Bonding (Berlin)* **1973**, *16*, 1–69. Christensen, J. J.; Eatough, D. J.; Izatt, R. M. *Chem. Rev.* **1974**, *74*, 351–384.

0002-7863/83/1505-4645$01.50/0